

DOE/PC/91307--T17



RICE

COAL COMBUSTION: EFFECT OF PROCESS CONDITIONS ON CHAR REACTIVITY

Quarterly Technical Report

Performance Period: 7/1/94 -9/30/94 (Quarter #12)

Submitted to the

Department of Energy

Grant Number DE-FG22-91PC91307

Grant Period: 9/1/1991 to 6/1/1995

PRINCIPAL INVESTIGATOR

Kyriacos Zygourakis

Department of Chemical Engineering

Rice University

Houston, Texas 77251-1892

DOE Technical Project Officer

Kamalendu Das

Morgantown Energy Technology Center

MASTER

RECEIVED
JSDOE/PETC
53 APR 21 PM 12:55
ACQUISITION ASSISTANCE DIV.

"U.S. DOE Patent Clearance is not required prior to the publication of this document"

THE ABOVE DOCUMENTS HAVE BEEN
ENTERED INTO THE DTS AND DISTRIBUTED
ON 5-8-95
THIS IS THE COPY FOR THE AWARD FILE.
DOCUMENT CONTROL CENTER

DISTRIBUTION OF THIS DOCUMENT IS UNLIMITED

el

DISCLAIMER

**Portions of this document may be illegible
in electronic image products. Images are
produced from the best available original
document.**

PROJECT OBJECTIVES

The project will quantify the effect of the following pyrolysis conditions on the macropore structure and on the subsequent reactivity of chars: (a) pyrolysis heating rate; (b) final heat treatment temperature (HTT); (c) duration of heat treatment at HTT (or soak time); (d) pyrolysis atmosphere (N_2 or O_2/N_2 mixtures); (e) coal particle size (100 - 1,000 μm in diameter); (f) sulfur-capturing additives (limestone); and (g) coal rank. Pyrolysis experiments will be carried out for three coals from the Argonne collection: (1) a high-volatile bituminous coal with high ash content (Illinois #6), (2) a bituminous coal with low ash content (Utah Blind Canyon) and (3) a lower rank subbituminous coal (Wyodak-Anderson seam).

Task A: We will obtain the time histories and follow the fate of single particles during pyrolysis in our TGA/VMI reactor. The experiments will be videotaped and digital images at several time instants will be acquired and analyzed on the image processor. For each run, we will measure particle swelling and shape, as well as the number and size of volatile bubbles evolving from each particle. For selected sets of conditions, several char samples will be collected and polished sections will be prepared so that we can accurately analyze the internal structure of the char particles. We will pay particular attention to the existence of correlations between particle swelling and macropore surface area as well as to the fate of ash inclusions during pyrolysis.

Task B: A different set of pyrolysis experiments will be immediately followed by combustion experiments. Without removing the particles from the TGA/VMI reactor, the char samples will be reacted with O_2 to complete conversion at high temperatures. Different gas flow rates of gases and O_2 concentrations will be used to investigate the effect of external mass transfer limitations. Issues to be addressed in this study will include the influence of particle swelling and ash content on thermal ignitions.

Task C: We will use mathematical models to simulate combustion of char particles in the regime of strong diffusional limitations. Digitized particle cross-sections obtained from our studies will be used as computational grids for these simulations and the average behavior will be obtained by analyzing a large number of particle cross-sections. The observed reactivity vs. conversion patterns will be analyzed and classified. These patterns will then be used in transient models to describe ignition and extinction phenomena in char combustion.

1. SUMMARY

A mathematical model was developed to study the thermal ignition of char particles. The model assumes a bimodal pores size distribution with small micropores (of the order of a few Å) and large micropores in the μm size range. All the model parameters can be estimated using data obtained previously in our laboratory. We are currently testing this model to determine its validity and to investigate how char properties (porosity, particle size, macropore surface area, micropore radius) and operating conditions (temperature, oxygen concentration, flow rate) affect ignition phenomena.

2. IGNITION OF CHAR PARTICLES

Several investigators have experimentally observed char ignition using different methods [1, 2, 3]. When combustion is observed with video microscopy, ignition appears as a luminous flame engulfing the char particle. The duration of the flame is in the order of one second. This phenomenon may appear on the reactivity plot as a "spike" or a sharp and sudden increase in the reaction rate for a small interval of conversion before the extinction happens. During this short time, a large amount of heat is released to the surrounding. Measurement of product gas concentration reveals that the concentration changes rapidly at the time of ignition [4]. Another experimental observation is that ignition is initiated in localized reactive spots on the particle surface and then propagates all over the entire surface [5]. More interestingly, at least two investigators have reported multiple ignitions on one particle. Up to a dozen multiple ignitions for some particles have been observed in our previous experimental work [6]. Solomon and coworkers [7] have observed a primary and then a more intense secondary ignition of particles injected into a hot gas stream. Until recently, however, few experimental studies attempted to quantify systematically the effects of process conditions (particle size, bulk concentration, and pyrolysis heating rate) on char ignition. Most of the results in this area come from theoretical studies.

The ignition phenomenon has been modeled in several ways. The Thermal Explosion Theory (TET), first formulated by Samenov, has been used to describe

both the heterogeneous and homogeneous ignitions [1, 8]. Briefly stated, the ignition happens when the heat generation curve (sigmoidal line) and the heat loss curve (straight line) intercept and the surface particle temperature takes the higher stable temperature. A more detail and specific model of coal ignition has been presented by Sotirchos and Amundson [9, 10, 11, 12] who developed a comprehensive model to simulate the reaction, mass and heat transfer in the particle and in the surrounding boundary layer.

The work of Sotirchos and Amundson predicts that there is a region of ambient temperatures where the solid temperature can take three steady-state values. The first is a stable steady state temperature that is slightly higher than the ambient. This is the situation when the oxygen penetrates the entire particle and reacts uniformly with the solid reactant. The second solution is unstable and the particle temperature is higher than the ambient. The third solution, which is stable, gives a particle temperature that is considerably higher than the ambient. In this case, the particle ignites homogeneously when carbon dioxide reacts with the carbon to produce carbon monoxide that burns in a sheath surrounding the particle. The model also predicts that larger particle size and larger pore radius reduce the ignition temperature.

The main parameters in ignition models are those describing the internal structure of the particles. In the absence of this information, the model may give qualitatively correct predictions but without satisfactory agreement with experiments. Therefore, it is important that we incorporate our accurate measurements of the pore structure of chars in any ignition model.

3. EXPERIMENTAL OBSERVATIONS OF CHAR PARTICLE IGNITIONS

When chars react with oxygen at low temperatures, oxygen can fully penetrate the micropores and the heterogeneous reactions take place in the kinetic control regime. Our measurements have shown that chars produced from Illinois #6 coal react with oxygen in the kinetic control regime at temperatures below 420 °C.

At higher temperatures, however, the rates of reaction and consumption of oxygen inside the particle are much faster than the rates of oxygen diffusion. In previous quarterly reports we have shown that 50-60 mesh char particles reacted with 33% oxygen at 550 °C exhibited the characteristic reactivity patterns (spikes)

indicating particle ignitions. Our video sequences showed that the ignited particles were engulfed in luminous flames that last for a fraction of a second. With chars produced from Illinois #6 coal particles in the 28-32 mesh size fraction, no ignitions were observed for combustion at 550 °C with 21% oxygen. The char reactivity patterns from some (but not all) combustion runs at 625 °C and 21% oxygen concentration showed rapid changes in the reaction rate indicating possible ignitions. The video tapes from these experiments, however, did not show particle ignitions with luminous flames. Only sudden and rapid consumption of char particles was observed on the video sequences. These results indicate that the rapidly consumed particles reacted at temperatures higher than the ambient temperature of 625 °C, but lower than the temperature required to produce a luminous flame. Finally, combustion runs at 550 °C and 33% oxygen gave reactivity patterns with sharp "spikes" indicating particle ignitions. These ignitions were confirmed from the video tapes.

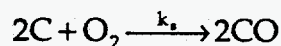
These experimental data led us to the conclusion that high oxygen concentrations increase the reaction rate and, consequently, the rate of heat generation inside the particle. When the rate of heat generation is substantially larger than the rate of heat removal from the particle, the particle temperature increases dramatically leading to thermal ignition. A luminous flame is observed if the particle temperature is high enough.

3. MODEL DEVELOPMENT

One of the objectives of TASK C of our project is to develop and test a steady-state mathematical model that can describe char particle ignitions. Results from macropore structure measurements of chars produced under different process conditions will be used to estimate all the model parameters. The model will then be used to systematically investigate the effect of porosity, particle size, macropore surface area, micropore radius, and the flow rate on ignition phenomena.

3.1 Heat and mass balances

Let us assume that the first order reaction



takes place in a spherical char particle with radius R . A detailed kinetic study conducted earlier in our laboratory revealed that the combustion reaction for the chars used here is first order with respect to oxygen concentration. If we assume that the concentration of gaseous reactant (oxygen) is uniform throughout the char particle, the steady-state mass balance is then given by

$$4\pi R^2 k_g (c_f - c_s) = \frac{4\pi R^3}{3} \eta k(T_s) c_s$$

or

$$k_g (c_f - c_s) = \frac{R}{3} \eta k(T_s) c_s \quad (1)$$

where c_f is the concentration of oxygen in the bulk phase, c_s is the concentration of oxygen in the reacting particle, k_g is the mass transfer coefficient, η is the effectiveness factor for the first order reaction and $k(T_s)$ is the reaction rate coefficient that depends on the solid temperature T_s according to

$$k(T_s) = k_0 e^{-\frac{E}{RT_s}}$$

The pre-exponential factor k_0 of the reaction rate expression and the activation energy E were measured in our laboratory and found to be 34.5 kcal/mol and $7.30 \times 10^7 \text{ sec}^{-1}$, respectively.

If we also assume uniform particle temperature, the steady-state heat balance becomes

$$4\pi R^2 h (T_s - T_f) = \frac{4\pi R^3}{3} (-\Delta H) \eta k(T_s) c_s$$

or

$$h (T_s - T_f) = \frac{R}{3} (-\Delta H) \eta k(T_s) c_s \quad (2)$$

where T_s is the particle temperature, T_g is the temperature of the ambient gas, h is the heat transfer coefficient and $(-\Delta H)$ is the heat of reaction (equal to 220.0 kJ/mol at standard conditions for our exothermic reaction).

Equation (1) can be solved for c_s to obtain:

$$c_s = \frac{k_g}{\frac{R}{3}\eta k_s + k_g} c_f \quad (3)$$

By substituting this expression for c_s in the heat balance of equation (2), the following algebraic equation is obtained:

$$Q_R \equiv \frac{3h}{Rk_g c_f} (T_s - T_f) = \frac{(-\Delta H)\eta k(T_s)}{\frac{R}{3}\eta k(T_s) + k_g} \equiv Q_G \quad (4)$$

The left hand side of the above equation gives the rate Q_R at which heat is removed from the char particle, while the right hand side gives the rate Q_G of heat generation. A straight line is obtained if we plot the heat removal function Q_r vs. T_s (at a fixed T_f), while a plot of Q_g vs. T_s yields a sigmoidal curve. The intersections of these two curves give the steady state solutions T_s of equation (4). The bisection method was used to solve the algebraic equation (4) for T_s at each T_f . Depending on the operating conditions and the ambient gas temperature T_f , there might exist one, two or three steady state solutions for equation (4).

3.2 Estimation of transport properties

Heat and mass transfer coefficients h and k_g were estimated using the correlations [13] for forced convection around a sphere given by

$$\frac{h(2R)}{k_f} = 2.0 + 0.6 Re^{1/2} Pr^{1/3} \quad (5)$$

and

$$\frac{k_g(2R)}{D_f} = 2.0 + 0.6 Re^{1/2} Sc^{1/3} \quad (6)$$

where the Reynolds, Prandtl and Schmidt numbers are defined by

$$Re = \frac{(2R)v_{\infty}\rho_f}{\mu_f} \quad (7)$$

$$Pr = \frac{c_{pf}\mu_f}{k_f} \quad (8)$$

$$Sc = \frac{\mu_f}{\rho_f D_f} \quad (9)$$

respectively, and where k_f is the bulk thermal conductivity, D_f is the bulk binary diffusion coefficient, v_{∞} is the velocity of the ambient gas flowing around the sphere, ρ_f is the bulk density, μ_f is the bulk viscosity, and c_{pf} is the heat capacity at constant pressure for the bulk gas. Using the above correlations, the model will also allow us to investigate the effects of ambient gas flow rates on ignition through the Reynolds number. In the case of stagnant fluid, the Reynolds number vanishes and the Nusselt and Sherwood numbers in equations (5) and (6) respectively reduce to 2.0.

Thermal conductivities of the pure gases are computed using a modified Eucken approximation [14] and the thermal conductivity of gas mixtures is estimated by a method suggested by Mason and Saxena [13]. Heat capacities are determined using the empirical equation given by Felder and Rousseau [15] and viscosities are calculated using the estimation presented by Thodos and coworkers (Perry, Green et al. 1984). The binary diffusion coefficients are estimated from the Fuller, Schettler, and Giddings relation [14].

3.3 Bimodal Pore Size Distribution and Effectiveness Factor

The effectiveness factor η must account for diffusional resistances in both the micropores and the macropores, since the pore structure of chars is characterized by a bimodal size distribution. For this purpose, the model proposed by Mingle and Smith [16, 17] is used. The mass balance for the micropores can be written as

$$D_{\mu} \frac{d^2 c_{\mu}}{dz^2} = \frac{2}{r_{\mu}} k_s c_{\mu} \quad (10)$$

where c_{μ} is the oxygen concentration in the micropores, z is the axial coordinate in the cylindrical micropores, D_{μ} is the diffusion coefficient for micropores, k_s is the surface reaction rate constant and r_{μ} is the average micropore radius. The boundary conditions for equation (10) are

$$\frac{dc_{\mu}}{dz} = 0 \quad @ z = 0$$

and (11)

$$c_{\mu} = c_M \quad @ z = L_{\mu}$$

where L_{μ} is the micropore length and c_M is the concentration at the end of the micropore where it opens up into a large macropore. Solving equation (10) with the boundary conditions (11) we obtain the effectiveness factor η_{μ} for the micropores:

$$\eta_{\mu} = \frac{\tanh \phi_{\mu}}{\phi_{\mu}} \quad (12)$$

where the Thiele modulus ϕ_{μ} is defined by

$$\phi_{\mu} = L_{\mu} \sqrt{\frac{2k_s}{r_{\mu} D_{\mu}}} \quad (13)$$

The size of the micropores L_{μ} is estimated as the ratio of volume to surface area of solid as follows

$$L_{\mu} = \frac{1 - \epsilon_M}{2S_g} \quad (14)$$

where S_g is the specific macropore surface area and ϵ_M is the macroporosity. The estimates obtained from equation (14) are valid when the average macropore size is large compared to the average micropore size. This is particularly true for the thin-walled chars produced at high pyrolysis heating rates.

The mass balance giving the concentration c_M of oxygen in the macropores becomes

$$D_e \frac{1}{r^2} \frac{d}{dr} \left(r^2 \frac{dc_M}{dr} \right) = \eta_\mu k(T_s) c_M \quad (15)$$

where r is the radial coordinate for the spherical particle and D_e is the effective diffusion coefficient for the macropores. The Thiele modulus in this case is

$$\phi_M = \frac{R}{3} \sqrt{\frac{\eta_\mu k(T_s)}{D_e}} \quad (16)$$

and the overall effectiveness factor η is

$$\eta = \eta_\mu \left[\frac{1 - (3\phi_M) \coth(3\phi_M) - 1}{\phi_M (3\phi_M)} \right] \quad (17)$$

or

$$\eta = \eta_\mu \eta_M \quad (18)$$

The diffusion coefficient D_μ in the micropores is calculated assuming Knudsen diffusion and the micropore radius r_μ is taken to be 5 Å since this is considered to be the size separating the micropores from submicropores. Our measurements of macropore radius reveal that the macropore radius is larger than 1000 Å. Therefore, the effective diffusion coefficient D_e can take the value of the bulk diffusion coefficient.

4. REFERENCES

1. Essenhigh, R. H., M. K. Misra and D. W. Shaw. "Ignition of coal particles: a review." *Combust. Flame.* 77(1): 3-30, 1989.
2. Tognotti, L., A. Malotti, L. Petarca and S. Zanelli. "Measurement of ignition temperature of coal particles using a thermogravimetric technique." *Combust. Sci. Technol.* 44(1-2): 15-28, 1985.

3. Zhang, D.-k., P. C. Hills, T. F. Wall and A. G. Tate. "The Ignition of Coal Particles and Explosions in Surrounding Combustible Gases During Heating by Laser Irradiation." *Fuel*. 71: 1206-1207, 1992.
4. Gomez, C. O. and F. J. Vastola. "Ignition and combustion of single coal and char particles. A quantitative differential approach." *Fuel*. 64(4): 558-63, 1985.
5. Levendis, Y. A., R. Sahu, R. C. Flagan and G. R. Gavalas. "Post-ignition transients in the combustion of single char particles." *Fuel*. 68(7): 849-55, 1989.
6. Matzakos, A. *Fundamental Mechanisms of Coal Pyrolysis and Char Combustion*. 1991.
7. Solomon, P. R., P. L. Chien, R. M. Carangelo, M. A. Serio and J. R. Markham. "New ignition phenomenon in coal combustion." *Combust. Flame*. 79(2): 214-15, 1990.
8. Semenov, N. "Zur Theorie des Verbrennungsprozesses." *Z. Physik*. 48: 571-582, 1928.
9. Sotirchos, S. V. and N. R. Amundson. "Diffusion and reaction in a char particle and in the surrounding gas phase. Two limiting models." *Ind. Eng. Chem. Fundam.* 23(2): 180-91, 1984.
10. Sotirchos, S. V. and N. R. Amundson. "Diffusion and reaction in a char particle and in the surrounding gas phase. A continuous model." *Ind. Eng. Chem. Fundam.* 23(2): 191-201, 1984.
11. Sotirchos, S. V. and N. R. Amundson. "Dynamic Behaviour of a Porous Char Particle Burning in an Oxygen-Containing Environment. Part I: Constant Particle Radius." *AIChE J.* 30(4): 537-549, 1984.
12. Sotirchos, S. V. and N. R. Amundson. "Dynamic Behaviour of a Porous Char Particle Burning in an Oxygen-Containing Environment. Part II: Transient Analysis of a Shrinking Particle." *AIChE J.* 30(4): 549-556, 1984.

13. Bird, R. B., W. E. Stewart and E. N. Lightfoot. "Transport Phenomena." 1960 John Wiley and Sons. New York.
14. Perry, R. H., D. W. Green and J. O. Maloney. "Perry's Chemical Engineers' Handbook." 1984 McGraw-Hill. New York.
15. Felder, R. M. and R. W. Rousseau. "Elementary Principles of Chemical Processes." 1978 John Wiley and Sons. New York.
16. Mingle, J. O. and J. M. Smith. "Effectiveness Factors for Porous Catalysts." *AIChE J.* 7(2): 243-249, 1961.
17. Froment, G. F. and K. B. Bischoff. "Chemical Reactor Analysis and Design." 1979 John Wiley and Sons. New York.

DISCLAIMER

This report was prepared as an account of work sponsored by an agency of the United States Government. Neither the United States Government nor any agency thereof, nor any of their employees, makes any warranty, express or implied, or assumes any legal liability or responsibility for the accuracy, completeness, or usefulness of any information, apparatus, product, or process disclosed, or represents that its use would not infringe privately owned rights. Reference herein to any specific commercial product, process, or service by trade name, trademark, manufacturer, or otherwise does not necessarily constitute or imply its endorsement, recommendation, or favoring by the United States Government or any agency thereof. The views and opinions of authors expressed herein do not necessarily state or reflect those of the United States Government or any agency thereof.
